11th International Symposium on Magnetic Bearings
August 26-29, Nara, Japan

ATTITUDE STABILIZATION CONTROL OF AMB-FLYWHEEL SUPPORTED BY TWO-AXES GIMBALS

Kenta Kuriyama
Dept. of Mech. Eng., Chiba Univ., 263-8522 Japan
ken-kuriyama@graduate.chiba-u.jp

Kenzo Nonami
Dept. of Mech. Eng., Chiba Univ., 263-8522 Japan
nonami@faculty.chiba-u.jp

Budi Rachmanto
Dept. of Mech. Eng., Chiba Univ., 263-8522 Japan
rac@graduate.chiba-u.jp

ABSTRACT

A flywheel energy storage system using magnetic bearing is one of effective methods to save electric power. Usually, we regard magnetic bearing as a system fixed to the environment. Then, we develop a vehicle with a flywheel energy storage system using the magnetic bearing and the gimbal. In this paper, we introduce mathematical model including not only flywheel but also gimbals. Also, it is verified through experiments that the proposed model is very effective in this paper.

INTRODUCTION

Now, global warming is one of important problem to solve. The important measure is creating the society without the fossil fuels.

Our study group is suggesting a flywheel energy storage system using magnetic bearing. And, we research stable control of this system. As a result, we achieve stability for this system fixed to the ground. But, this result is not the condition for on the vehicle. Then, we research a mobile flywheel energy storage system using magnetic bearing on a vehicle.

For this purpose, the vehicle in Fig.1 is choosed. This vehicle is a small and light electric car, and has already equipped with energy regeneration system. Research concludes that a flywheel energy storage system using the magnetic bearing needs the gimbal system in this case. But, the literature treating this system are nothing. We need to derive the equation of this system.

This paper introduces mathematical model not only flywheel but also gimbal and analyze this model.

FIGURE 1: Electric vehicle as platform

GIMBAL SYSTEM

The gimbal system is in Fig.2. This gimbal system is hidden under the rear seat of the vehicle. This gimbal has two degree, an angle around the front direction and a vertical angle of the above angle. And including the part of the frame of the vehicle as the part of the gimbal system, the gimbal system become smaller and lighter.

In the case which a flywheel using the magnetic bearing fixed on the vehicle, flywheel rotor lean by the acceleration and the deceleration of the vehicle. Without gimbal system, the casing of the flywheel system does not lean. So, the flywheel rotor touches the bearing (touch-down) and uses more control energy. By the research about this effect is confirmed that our flywheel using the magnetic bearing is not fit to use on the vehicle by the simulations.

Now consider the using the gimbal system. With gimbal, not only flywheel rotor but also the casing lean by the acceleration and the deceleration of the vehicle. So, there is a possibility that the flywheel rotor does not touch with the casing. Because of

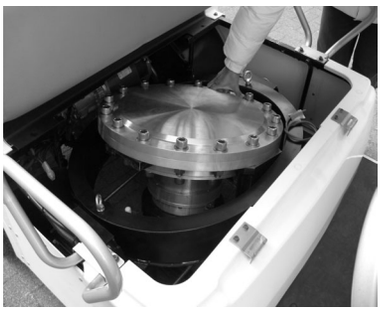

FIGURE 2: Gimbal system

this, using the gimbal system with a flywheel using the magnetic bearing is decided.

FLYWHEEL SYSTEM

The flywheel system is in Fig.3 and Fig.4 Now, we achieve the stability for this system with PID gains scheduling with the PID gains in Table2.

RIGID MODEL

The regid model is derived from the equation about the center of gravity. The means of the signs in Table1 are below.

- G : The position of the center of gravity of the rotor
- L_u, L_l:The distance between the center of gravity and magnets
- L : $L = L_l - Lu$
- $I_1 \sim I_8$: Control current
- x_g,x_u,x_l : Center of gravity of the rotor in X-Z space, displacement of rotor at upper and lower magnets
- ω : Angular velocity
- θ_x,θ_y: Angular displacement

Eq.(1) are the mathematical model including the effect of the gyro and unbalance oscillation.

$$\begin{cases} M\ddot{x}_g = F_{xu} + F_{xl} + M\delta\omega^2 \cos\omega t \\ I_r\ddot{\theta}_y = F_{xu}L_u + F_{xl}L_l - \omega I_z\dot{\theta}_x + l_c M\delta\omega^2 \cos\omega t \\ M\ddot{y}_g = F_{yu} + F_{yl} + M\delta\omega^2 \sin\omega t \\ I_r\ddot{\theta}_x = F_{yu}L_u + F_{yl}L_l + \omega I_z\dot{\theta}_y + l_c M\delta\omega^2 \sin\omega t \end{cases} \quad (1)$$

The relation between the displacement of the sensor and the displacement of the center of gravity and the angle of the rotor are below.

$$\begin{cases} X_u = x_g + L_u\theta_y \ , & X_l = x_g + L_l\theta_y \\ Y_u = y_g + L_u\theta_x \ , & Y_l = y_g + L_l\theta_x \end{cases} \quad (2)$$

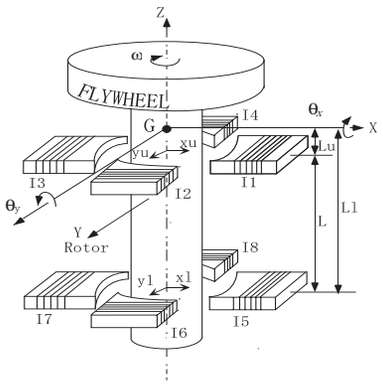

FIGURE 3: Model of the AMB with flywheel

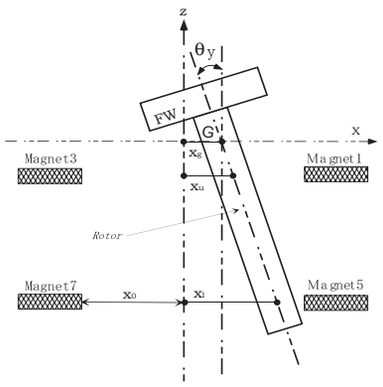

FIGURE 4: Schematic diagram of X-Z plane

Then, the equation about the center of gravity $\dot{x} = Ax + BU + E(\omega)$ and the output equation are below. State quantity x is the displacement and the velocity of the center of gravity. $x = [x_1 \ x_2]^t, x_1 = [x_g \quad \theta_y \quad y_g \quad \theta_x]^t, x_2 = [\dot{x_g} \quad \dot{\theta_y} \quad \dot{y_g} \quad \dot{\theta_x}]^t$, The control inputs $U = [F_{xu} \quad F_{xl} \quad F_{yu} \quad F_{yl}]^t$ are the suction between the magnets.

$$\begin{pmatrix} \dot{x}_1 \\ \dot{x}_2 \end{pmatrix} = \begin{pmatrix} 0_{4\times4} & I_{4\times4} \\ 0_{4\times4} & A_{22}(\omega) \end{pmatrix} \begin{pmatrix} x_1 \\ x_2 \end{pmatrix} + \begin{pmatrix} 0_{4\times4} \\ B_2 \end{pmatrix} U + \begin{pmatrix} 0_{4\times2} \\ E_2 \end{pmatrix} \begin{pmatrix} \cos(\omega t) \\ \sin(\omega t) \end{pmatrix} \quad (3)$$

$$Y = \begin{pmatrix} X_u \\ X_l \\ Y_u \\ Y_l \end{pmatrix}$$

$$= \left(\begin{array}{cccc|c} 1 & L_u & 0 & 0 & 0_{1\times4} \\ 1 & L_l & 0 & 0 & 0_{1\times4} \\ - & - & - & - & - \\ 0 & 0 & 1 & L_u & 0_{1\times4} \\ 0 & 0 & 1 & L_l & 0_{1\times4} \end{array} \right) \left(\begin{array}{c} x_1 \\ x_2 \end{array} \right) \tag{4}$$

Then,,

$$A_{22}(\omega) = \left(\begin{array}{cccc} 0 & 0 & 0 & 0 \\ 0 & 0 & 0 & -\omega I_z/I_r \\ 0 & 0 & 0 & 0 \\ 0 & -\omega I_z/I_r & 0 & 0 \end{array} \right)$$

$$B_2 = \left(\begin{array}{cccc} 1/M & 1/M & 0 & 0 \\ L_u/I_r & L_l/I_r & 0 & 0 \\ 0 & 0 & 1/M & 1/M \\ 0 & 0 & L_u/I_r & L_l/I_r \end{array} \right)$$

$$E2 = \left(\begin{array}{cc} \delta\omega^2 & 0 \\ l_c\delta\omega^2 & 0 \\ 0 & \delta\omega^2 \\ 0 & l_c\delta\omega^2 \end{array} \right)$$

COORDINATE TRANSFORMATION

By Eq.(2), relations between state quantity of the model about the center of gravity and the displacement of the sensor become below.

$$\left(\begin{array}{c} x_g \\ \theta_y \\ y_g \\ \theta_x \end{array} \right) = T \left(\begin{array}{c} X_u \\ X_l \\ Y_u \\ Y_u \end{array} \right) \tag{5}$$

$$T = \left(\begin{array}{cccc} L_l/L & -Lu/L & 0 & 0 \\ -1/L & 1/L & 0 & 0 \\ 0 & 0 & L_l/L & -Lu/L \\ 0 & 0 & -1/L & 1/L \end{array} \right)$$

And

$$x = GX', \quad G = \left(\begin{array}{cc} T & 0 \\ 0 & T \end{array} \right) \tag{6}$$

Then, Eq.(3) transforms into Eq.(7).

$$\left\{ \begin{array}{l} \dot{X'} = \bar{A}X' + \bar{B}U + \bar{E}(\omega) \\ \bar{A} = G^{-1}AG, \ \bar{B} = G^{-1}B \\ \bar{E} = G^{-1}E \end{array} \right. \tag{7}$$

$X' = [x'_1 \ x'_2]^t, x'_1 = [X_u \ X_l \ Y_u \ Y_l]^t, \ x'_2 = \dot{x'_1}$. The parameters used in this section in Tablel1. But, $M = M_r + M_f$.

TABLE 1 Parameters of flywheel rotor-AMB

Item	Value
Mass of rotor (M_r)	4.85[kg]
Mass of flywheel (M_f)	8.82[kg]
Moment of interia about z axis (I_z)	1.86 $\times 10^{-1}$ $[kgm^2]$
Moment of interia about x and y axis (I_r)	1.73 $\times 10^{-1}$ $[kgm^2]$
Constant of upper magnetic attractive force (K_u)	3.10 $\times 10^{-6}$ $[Nm^2/A^2]$
Constant of lower magnetic attractive force (K_l)	4.47 $\times 10^{-6}$ $[Nm^2/A^2]$
Distance from the center of the gravity ($upper : L_u$)	4.99 $\times 10^{-2}[m]$
Distance from the center of the gravity ($lower : L_l$)	1.67 $\times 10^{-1}[m]$
Nominal air gap $(X_0), (Y_0)$	0.25 $\times 10^{-3}[m]$
Bias Current(I_0)	0.3 $[A]$

TABLE 2 Gains of PID contoller

f[Hz]	k_d	k_p	k_i
0-20	4×10^3	2×10^6	4×10^6
20-45	3.8×10^3	1.8×10^6	0.5×10^6
45-100	3.5×10^3	1.5×10^6	0.3×10^6
100-150	3×10^3	0.9×10^6	0.25×10^6
150-200	2.5×10^3	0.9×10^6	0.25×10^6
200-240	2.3×10^3	0.8×10^6	0.2×10^6
240-300	0.2×10^3	0.8×10^6	0.2×10^6

MODELING OF FLYWHEEL AND GIMBAL

Next, the deriving the equation including a AMB-flywheel system and the gimbal system with the Lagrangian equation is treated. And, for easy way, supposed that the gimbal system is fixed on the ground.

First definitions θ_i (the leans of the inner gimbal) and θ_y (the leans of the outer gimbal) are the leans of the gimbal system in Fig.5. Second definitions θ_x and θ_y in Fig.3 and Fig.4 are the leans from the gimbal. Then, the kinetic energy of whole system T and the potential energy of whole system U are below.

$$\left\{ \begin{array}{l} T = \frac{1}{2}M(\dot{x_g}^2 + \dot{y_g}^2) \\ \qquad +\frac{1}{2}I_r\{(\dot{\theta}_x + \dot{\theta}_i)^2 + (\dot{\theta}_y + \dot{\theta}_o)^2\} \\ \qquad +\frac{1}{2}I_i\dot{\theta}_i^2 + \frac{1}{2}I_o\dot{\theta}_o^2 + \frac{1}{2}I_z\omega^2 \\ U = -Mg\{x_g \sin(\theta_x + \theta_i) + y_g \sin(\theta_y + \theta_0)\} \end{array} \right. \tag{8}$$

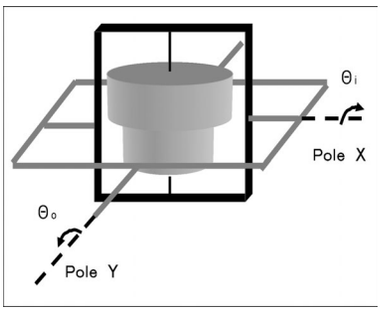

FIGURE 5: Co-ordinates of gimbal system

I_i, I_o are the moment of inertia about each rotaion. And, ω is below.

$$\omega = \dot{\theta}_z + (\dot{\theta}_y + \dot{\theta}_o)\cos(\theta_x + \theta_i) \tag{9}$$

From these, we use the Lagrangian equation for each x_g, θ_y, y_g, θ_x, θ_o, θ_i. And, considering the input of attitude control, Eq.(10) is obtained.

$$\begin{cases} M\ddot{x}_g - Mg\sin(\theta_y + \theta_o) = F_{xu} + F_{xl} \\ I_r(\ddot{\theta}_y + \ddot{\theta}_o) - \omega I_z(\dot{\theta}_x + \dot{\theta}_i)\sin(\theta_x + \theta_i) \\ \quad -Mgx_g\cos(\theta_y + \theta_o) = F_{xu}L_u + F_{xl}L_l \\ M\ddot{y}_g - Mg\sin(\theta_x + \theta_i) = F_{yu} + F_{yl} \\ I_r(\ddot{\theta}_x + \ddot{\theta}_i) + \omega I_z(\dot{\theta}_y + \dot{\theta}_o)\sin(\theta_x + \theta_i) \\ \quad -Mgy_g\cos(\theta_x + \theta_i) = F_{yu}L_u + F_{yl}L_l \\ I_r\ddot{\theta}_y + (I_r + I_o)\ddot{\theta}_o - \omega I_z(\dot{\theta}_x + \dot{\theta}_i)\sin(\theta_x + \theta_i) \\ \qquad -Mgx_g\cos(\theta_y + \theta_o) = 0 \\ I_r\ddot{\theta}_x + (I_r + I_i)\ddot{\theta}_i + \omega I_z(\dot{\theta}_y + \dot{\theta}_o)\sin(\theta_x + \theta_i) \\ \qquad +Mgy_g\cos(\theta_x + \theta_i) = 0 \end{cases} \tag{10}$$

Eq.(10) transforms to Eq.(11).

$$\begin{cases} M\ddot{x}_g = Mg\sin(\theta_y + \theta_o) + F_{xu} + F_{xl} \\ I_r\ddot{\theta}_y = \omega I_z(\dot{\theta}_x + \dot{\theta}_i)\sin(\theta_x + \theta_i) \\ \quad +Mgx_g\cos(\theta_y + \theta_o) + (1 + \frac{I_r}{I_o})(F_{xu}L_u + F_{xl}L_l) \\ M\ddot{y}_g = Mg\sin(\theta_x + \theta_i) + F_{yu} + F_{yl} \\ I_r\ddot{\theta}_x = -\omega I_z(\dot{\theta}_y + \dot{\theta}_o)\sin(\theta_x + \theta_i) \\ \quad +Mgy_g\cos(\theta_x + \theta_i) + (1 + \frac{I_r}{I_i})(F_{yu}L_u + F_{yl}L_l) \\ I_o\ddot{\theta}_o = -F_{xu}L_u - F_{xl}L_l \\ I_i\ddot{\theta}_i = -F_{yu}L_u - F_{yl}L_l \end{cases} \tag{11}$$

In Eq.(11), the damping of the gimbal system is not considered. Then, the damping of the gimbal system in Eq.(11) is considered with the experimental results, Fig.6 and Fig.7 with supposition that the oscillation damps as the index function

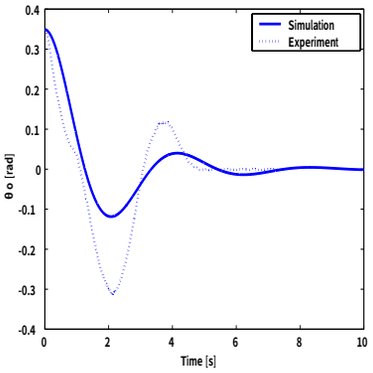

FIGURE 6: Time history response of outer gimbal

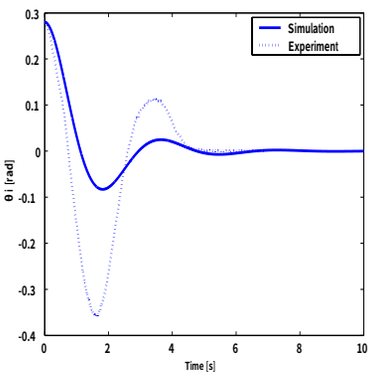

FIGURE 7: Time history response of inner gimbal

$$\begin{cases} M\ddot{x}_g = Mg\sin(\theta_y + \theta_o) + F_{xu} + F_{xl} \\ I_r\ddot{\theta}_y = \omega I_z(\dot{\theta}_x + \dot{\theta}_i)\sin(\theta_x + \theta_i) \\ \quad +Mgx_g\cos(\theta_y + \theta_o) \\ \quad +(1 + \frac{I_r}{I_o})(F_{xu}L_u + F_{xl}L_l) \\ M\ddot{y}_g = Mg\sin(\theta_x + \theta_i) + F_{yu} + F_{yl} \\ I_r\ddot{\theta}_x = -\omega I_z(\dot{\theta}_y + \dot{\theta}_o)\sin(\theta_x + \theta_i) \\ \quad +Mgy_g\cos(\theta_x + \theta_i) \\ \quad +(1 + \frac{I_r}{I_i})(F_{yu}L_u + F_{yl}L_l) \\ I_o\ddot{\theta}_o = -2\zeta_o\omega_{no}\dot{\theta}_o - {\omega_{no}}^2\theta_o - F_{xu}L_u - F_{xl}L_l \\ I_i\ddot{\theta}_i = -2\zeta_i\omega_{ni}\dot{\theta}_i - {\omega_{ni}}^2\theta_i - F_{yu}L_u - F_{yl}L_l \end{cases} \tag{12}$$

In Eq.(12), $\zeta_o = 0.26$, $\omega_{no} = 1.6$[rad/s], $\zeta_i = 0.29$, $\omega_{ni} = 1.85$[rad/s].

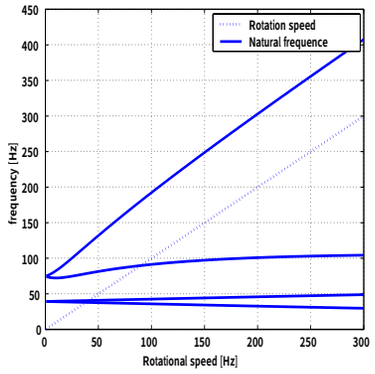

FIGURE 8: Natural frequence of flywheel rotor without gimbal

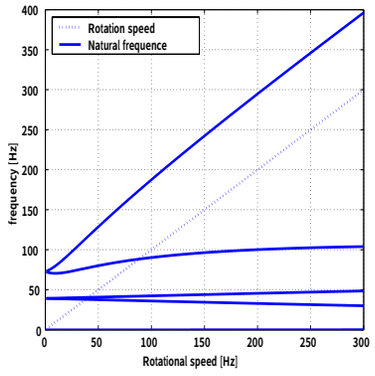

FIGURE 9: Natural frequence of flywheel rotor with gimbal

SIMULATION AND EXPERIMENT

NATURAL FREQUENCY COMPARISON

For examining the effect of the gimbal system, the natural frequencies of Eq.(1) and Eq.(12) are compared. In this comparison, the attitude control to each rotational speed is not effective. Only the PID gains at 0[Hz] in Table2 is used from 0[Hz] and 300[Hz]. The results are in Fig.8, Fig.9. In the simulation, the natural frequence at 0[Hz] decreases from 77[Hz] to 69[Hz] and from 34[Hz] to 30[Hz] in Fig.8 and Fig.9. In the experiment, the natural frequence at 0[Hz] decrease from 80[Hz] to 58[Hz] and from 22[Hz] to 15[Hz]. This effect comes from that the gimbal system works as the vibration absorber. And in Fig.9, the simulation result accords with the experiment result.

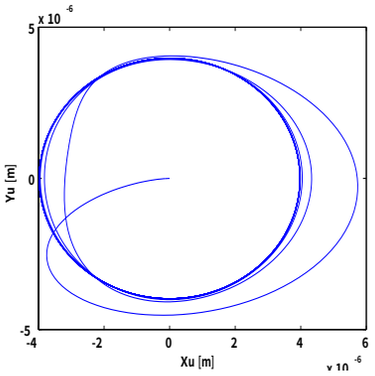

FIGURE 10: Orbit of upper side of rotor (20[Hz])

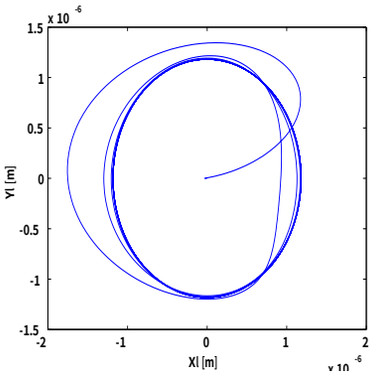

FIGURE 11: Orbit of lower side of rotor (20[Hz])

ORBIT COMPARISON

Next compare is the orbit of Eq.(1) and Eq.(12). The results are below.

First, the results at 20[Hz] are from Fig.10 and Fig.13. In this case, Eq.(12) is narrower than Eq.(1) at the point of the orbit width. This effect shows that the attitude control is effective in the case the rotor leans.

Next, the results at 120[Hz] are from Fig.14 and Fig.17. In this case, Eq.(12) is narrower than Eq.(1) at the point of the orbit width, too.

COMPARISON IN CASE VEHICLE ACCELERATION

The comparisons the simulation with the experiment in the case vehicle acceleration are in Fig.18 and Fig.19. In the experiment, the vehicle velocity is about 7[km/h] and rotor rotation speed is about 10[Hz].

In Fig.18, the fundamental wave in the simulation result vibrates. But, the experoment result does not vibrate like the simulation result. This difference comes from the air friction. Air friction works as

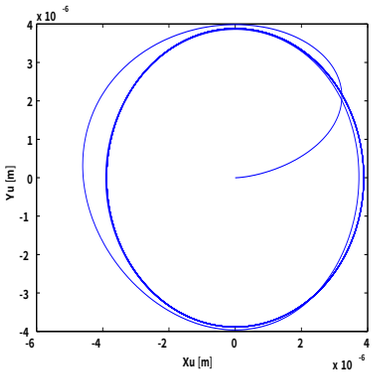

FIGURE 12: Orbit of upper side of rotor (with gimbal,20[Hz])

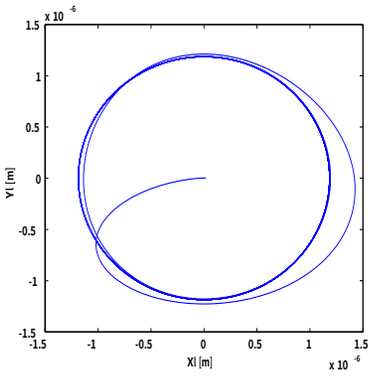

FIGURE 13: Orbit of lower side of rotor (with gimbal,20[Hz])

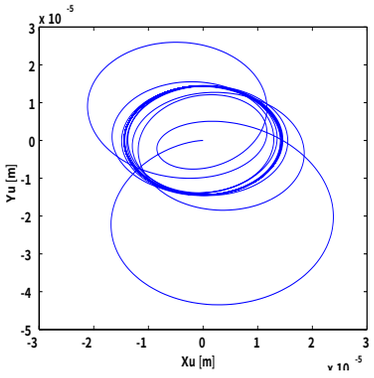

FIGURE 14: Orbit of upper side of rotor (120[Hz])

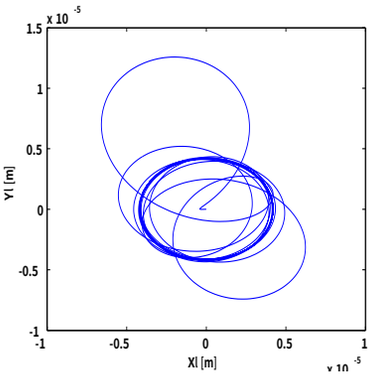

FIGURE 15: Orbit of lower side of rotor (120[Hz])

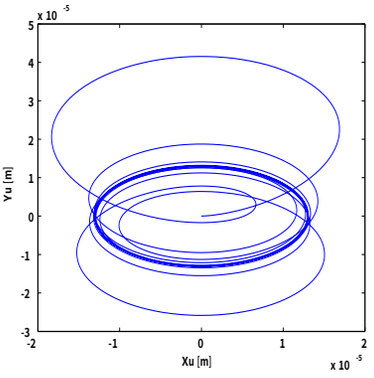

FIGURE 16: Orbit of upper side of rotor (with gimbal,120[Hz])

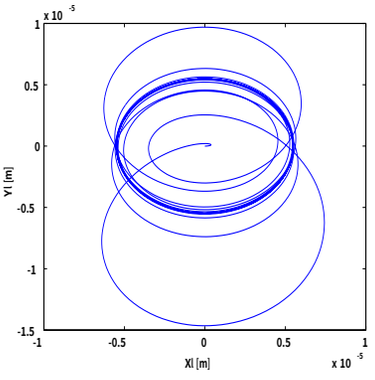

FIGURE 17: Orbit of lower side of rotor (with gimbal,120[Hz])

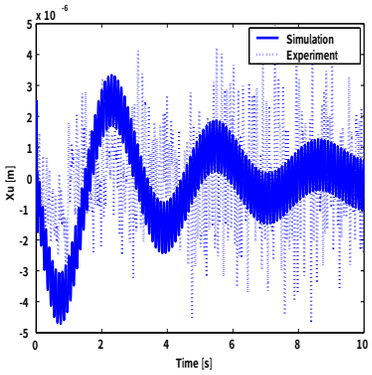

FIGURE 18: Time history response of X_u in case vehicle accelerate

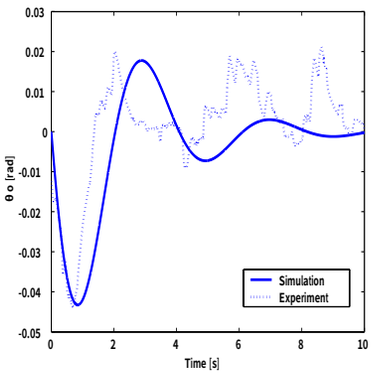

FIGURE 19: Time history response of θ_o in case vehicle accelerate

the shock absorber in the experiment. In this point, the air friction is pleasant. But, it interferes with high speed rotation. So, usually the vacuum pump is used and makes the vaccum in the casing. And, the experiment result is wider than the simulation result. For this, there are some improvement points in the mathematical model.

In Fig.19, there is the difference from 5[s] to 10[s]. This difference comes from the vehicle acceleration. In this comparison, Fig.19 is the result by the impulse input to the vehicle acceleration. But, the experiment acceleration is not strictly. For this, there are the difference. Except this difference, the simulation result resembles the experiment result.

CONCLUSIONS

This paper derived mathematical model including flywheel using magnetic bearing and gimbals systems.

And, first comparison was about the natural freqencies. The result was that using the gimbal system makes the natural freqencies lower. And, in this pint, the gimbal system was effective.

Next comparison was the orbits at 20[Hz] and 120[Hz]. The result was that the orbits with the gimbal system was narrower than the orbits without the gimbal system at the point of the orbit width. In this pint, the gimbal system was effective, too.

Last comparison was the result in the case vehicle acceleration. Approximatelly, the simulation result was near the experiment result. In this point, the mathematical model was effective.

Through three comparisons, the validity of the gimbal system was developed.

Hereafter, the experiment that the case rotor rotate high speed or that the vehicle suddenly accelerate and decelerate are necessary. And the improvement of the mathematical model, for example, about the the supposition that the oscillation damps as the index function, is necessary, too.

REFERENCES

1. Shimada, R., Flywheel Energy Storage System, Journal of the Japan Society of Mechanical Engineers,Vol.97, pp.948-949 (1994)

2. Saito, T. and Ogasawara, H.and Yamada, N., Study of Flywheel Energy Storage System and Application to Electric Vehicle, Transactions of the Japan Society of Mechanical Engineers. B,Vol.70, pp.2482-2489 (2004)

3. Nakai, H., and Matsuda, A. and Suzuki, M., Development of the Suspensions for the Flywheel Energy Storage System —Design and Testing of the Controller for the Gimbal—, Transactions of the Japan Society of Mechanical Engineers. C, Vol.66, pp.67-73 (2000)

4. Ariga, Y. and Nonami, K. and Ueyama, H., Nonlinear zero power control of energy storage flywheel system : Derivation of nonlinear control system without gyroscopic effects : Journal of the Japan Society of Applied Electromagnetics, Vol,8, pp.403-410 (2000)

5. Yokota, S. and Nishijima, T. and Kondoh, Y. and Kita, Y., A Flywheel Hybrid Vehicle Making Use of Constant Pressure System —Fabrication of Sationary Test Facility and Experiment of Urban Driving Schedule—, Transactions of the Japan Society of Mechanical Engineers. C, Vol.68, pp.2127-2132 (2002)

6. Otaki, H. amd Kosuda, M., Some Analyses and Development of Flywheel Powered Vehicle, Transactions of the Japan Society of Mechanical Engineers. C, Vol.46, pp.1375 (1980)

7. Ronald N. Arnold, Leonard Maunder：Gyrodynamics and its engineering applications, Academic Press (1961)

8. R.Gasch, H.Pfutzner：Rotordynamik, Berlin・Heidelberg・New York (1975)